



Reduction Data Obtained from Cyclic Voltammetry of Benzophenones and Copper-2-Hydroxyphenone Complexes

Emmie Chiyindiko¹, Ernst H. G. Langner^{1,*}  and Jeanet Conradie^{1,2,*} ¹ Department of Chemistry, University of the Free State, Bloemfontein 9300, South Africa² Department of Chemistry, UiT-The Arctic University of Norway, N-9037 Tromsø, Norway

* Correspondence: langneeh@ufs.ac.za (E.H.G.L.); conradj@ufs.ac.za (J.C.)

Abstract: This article provides detailed redox data on nine differently substituted benzophenones and ten square planar copper(II) complexes containing 2-hydroxyphenones obtained by cyclic voltammetry (CV) experiments. The information provided is related to the published full research articles “An electrochemical and computational chemistry study of substituted benzophenones” (*Electrochim. Acta* **2021**, *373*, 137894) and “Electrochemical behaviour of copper(II) complexes containing 2-hydroxyphenones” (*Electrochim. Acta* **2022**, *424*, 140629), where the CVs and electrochemical data at mainly one scan rate, namely at 0.100 Vs⁻¹, are reported. CVs and the related peak current and voltage values, not reported in the related research article, are provided in this article for nine differently substituted benzophenones and ten differently substituted copper-2-hydroxyphenone complexes at various scan rates over more than two orders of magnitude. The redox data presented are the first reported complete set of electrochemical data of nine 2-hydroxyphenones and ten copper(II) complexes containing 2-hydroxyphenone ligands.

Dataset: 10.38140/ufs.21731591; 10.38140/ufs.21731636**Dataset License:** CC-BY**Keywords:** benzophenone; copper-2-hydroxyphenone; reduction; cyclic voltammetry

Citation: Chiyindiko, E.; Langner, E.H.G.; Conradie, J. Reduction Data Obtained from Cyclic Voltammetry of Benzophenones and Copper-2-Hydroxyphenone Complexes. *Data* **2022**, *7*, 183. <https://doi.org/10.3390/data7120183>

Academic Editor: Igor I. Baskin

Received: 20 October 2022

Accepted: 13 December 2022

Published: 19 December 2022

Publisher's Note: MDPI stays neutral with regard to jurisdictional claims in published maps and institutional affiliations.



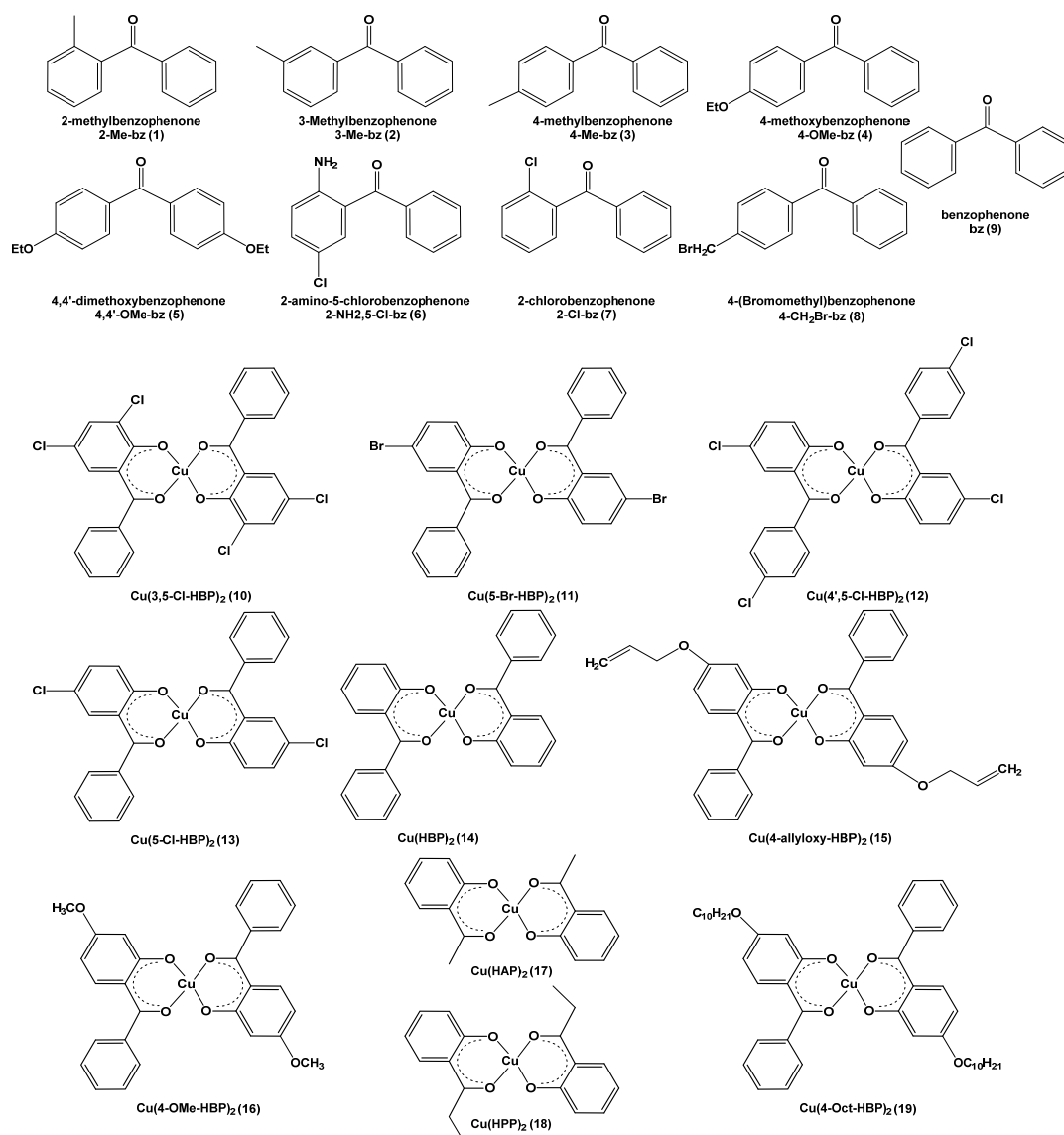
Copyright: © 2022 by the authors. Licensee MDPI, Basel, Switzerland. This article is an open access article distributed under the terms and conditions of the Creative Commons Attribution (CC BY) license (<https://creativecommons.org/licenses/by/4.0/>).

1. Summary

More than 300 natural benzophenones with a large variety in structure and biological activities exist [1]. Both natural and synthetic benzophenones are continuously being tested as potential sources of new drugs for their cytotoxicity and effects on cancer cells, antibacterial activity, antimicrobial activity, antifungal activity, antioxidant activity, anti-viral activity, anti-parasitic activity, anti-inflammatory activity, anti-anaphylactic activity, hepatoprotective activity, anti-diabetic, and vascular effects [1]. Since benzophenone derivatives absorb UV light, they are used as a UV curing agent in coating additives, plastics [2], and ink [3]. Oxybenzophenone is widely used as a UV filter in sunscreens and many other personal care products and cosmetics [4]. Benzophenones showed good performance as an anolyte in organic redox flow batteries [5]. In all applications, knowledge of benzophenones' stability against reduction is important. The many industrial applications of benzophenone lead to pollution risk [6]. Therefore, the reduction potentials of benzophenones are needed to determine if oxidising or reducing conditions are favoured in water or soil.

Redox data obtained from cyclic voltammetry of differently substituted benzophenones and copper(II) complexes containing 2-hydroxyphenones are provided in the article. Redox data are important for many applications, including energy storage devices (batteries), photographic processing, energy production, photosynthesis, respiration, combustion, corrosion, extraction of metals from polluted water, production of chemicals, and medicine. Information regarding peak current and voltage values obtained from cyclic voltammetry experiments are reported at only one scan rate (normally 0.100 V s⁻¹), and no, or only

selected, cyclic voltammograms (CVs) are shown. The advantage of having redox data and the related cyclic voltammograms at different scan rates is to (i) to ensure that the observed electrochemical behaviour at 0.100 V s^{-1} does not change at higher scan rates, (ii) to be able to determine if the reduction process is diffusion-controlled by application of the Randles–Ševčík equation, and (iii) to be able to determine diffusion coefficients of the analyte by application of the Randles–Ševčík equation (important for understanding the reactivity of the species under investigation). Apart from the related research articles [7,8], the limited reported scan rate data on substituted benzophenones and copper-2-hydroxyphenone complexes are available, as will be explained in the next two paragraphs. Therefore, this article provides CVs and reports the cyclic voltammetry peak current and voltage values (at scan rates over 2 orders of magnitude) of the reduction of nine substituted benzophenones and ten copper(II) complexes containing 2-hydroxyphenones, shown in Scheme 1.



Scheme 1. Naming, numbering, and structure benzophenones (1–9) and copper-2-hydroxyphenone complexes (10–19).

While the redox behaviour obtained from cyclic voltammograms of benzophenone in non-aqueous solvents is well-reported in the literature [9–15], only a few reports could be found on the redox data obtained from cyclic voltammograms on substituted benzophenones. One article provided redox data obtained from cyclic voltammograms (with-

out showing the CVs) of *ortho* and *para* methyl and tertiary butyl substituted benzophenones [11]. Another article reported cyclic voltammetry data (showing selected CVs at one scan rate) of halogen-substituted benzophenones [16]. A third article provided redox data obtained from cyclic voltammograms of four benzophenones (showing the CV of only benzophenone at one scan rate) [17]. A fourth article mentioned the reduction potential of benzophenone and two *para*-substituted benzophenones [5]. While comprehensive electrochemical data on hydroxybenzophenones are available [18–20], no comprehensive scan rate study on the redox behaviour of benzophenone or other substituted benzophenones could be found in the literature, except that for benzophenone and 2-amino-5-nitrobenzophenone reported in the related research article [7]. Due to limited reported scan rate studies on substituted benzophenones, in this article, we provide CVs and electrochemical data describing the chemical and electrochemical reversibility of the benzophenone/[benzophenone^{•-}]⁻ redox couple. Results on the peak current ratio, peak current voltage separation, and relationship between peak current and the square root of the scan rate are presented. The benzophenones contain different substituent groups. To determine the influence of electron donating and electron withdrawing groups on the reduction potential of benzophenone, see Scheme 1. The shift in the reduction potential of the first reversible reduction peak of the benzophenones presented here, Figure 1, demonstrates the dependence of the reduction process on the position and type of substituents on the aromatic rings of the benzophenone, also confirming that there is excellent communication between the benzophenone backbone and the various substituent groups. In this article, a large amount of data not reported in the related research article, “An electrochemical and computational chemistry study of substituted benzophenones” [7] are, thus, presented.

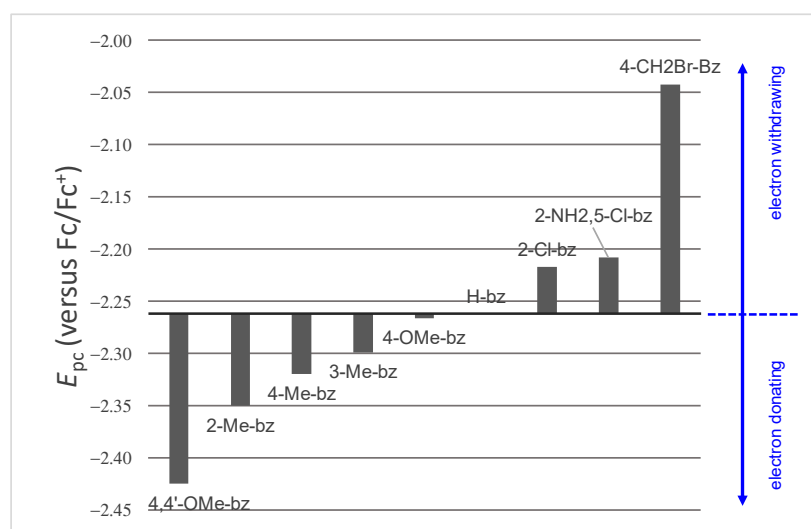


Figure 1. Reduction potential of benzophenones (1–8) containing electron-donating (CH₃, OCH₃, NH₂) and electron withdrawing (Cl, CH₂Br) groups, relative to unsubstituted benzophenone (H-bz, 9). Data were obtained at a scan rate of 0.100 V s⁻¹ in dimethylformamide as solvent from the related research article [1].

Regarding the copper-2-hydroxyphenone complexes, again, limited results are available in the literature on the synthesis, characterization, and redox properties of these copper(II) complexes containing 2-hydroxyphenones [21–23]. Except for the related research article [8], electrochemical results of only one of the complexes of this study, namely of Cu(HBP)₂ (14), at only one scan rate (no CV shown), are available in the literature [22]. Due to the limited published CVs and reduction data on these complexes, this article also provides CVs, current-voltage values and extensive electrochemical information obtained at eleven different scan rates varying from 0.02 V s⁻¹ to 10.24 V s⁻¹ (500 times increase in scan rate), for ten copper(II) complexes containing 2-hydroxyphenones, see Scheme 1 for

the complexes. The CVs obtained for the Cu(II/I) reduction are similar to those obtained for related square planar ($\text{Cu}^{\text{II}}(\beta\text{-diketonato})_2$) complexes, also containing two bidentate ligands with oxygen donor atoms, that form 6-membered rings with copper [24–28]. The reduction of a square planar Cu(II) complex leads to a tetrahedral Cu(I) complex [29]. The distortion in the geometry upon reduction could be a reason for the quasi-reversible to irreversible nature of the Cu(II/I) redox process. This article provides a large amount of data, obtained at different scan rates, not previously reported in the literature or in the related research article “Electrochemical behaviour of copper(II) complexes containing 2-hydroxyphenones” [8], where electrochemical data obtained at a scan rate of 0.100 V s^{-1} are provided and a few selected CVs are shown.

2. Data Description

Molecules containing electron-donating groups and ligands are oxidised at a lower potential than molecules containing electron-withdrawing groups and ligands. The influence of different electron donating and electron withdrawing groups on the reduction potential of structure benzophenones (1–9) and copper-2-hydroxyphenone complexes (10–19) are shown in Figures 1 and 2, respectively. This trend is as expected and in agreement with the trends observed for the reduction of enolised 1,3-diketones [30], *para*-substituted nitrobenzenes [31], bis(cyclopentadienyl)mono(β -diketonato) titanium(IV) complexes [32,33], tris(β -diketonato)metal(III) complexes (metal = Co [34], Cr [35], Mn [36], and Fe [37]), and octahedral bis(β -diketonato)-titanium(IV) complexes [38]. The amount of shift to lower (due to electron-donating substituents) or higher (due to electron-withdrawing substituents) potentials, however, depends on the resonance and inductive electronic effects of the substituents [31,39].

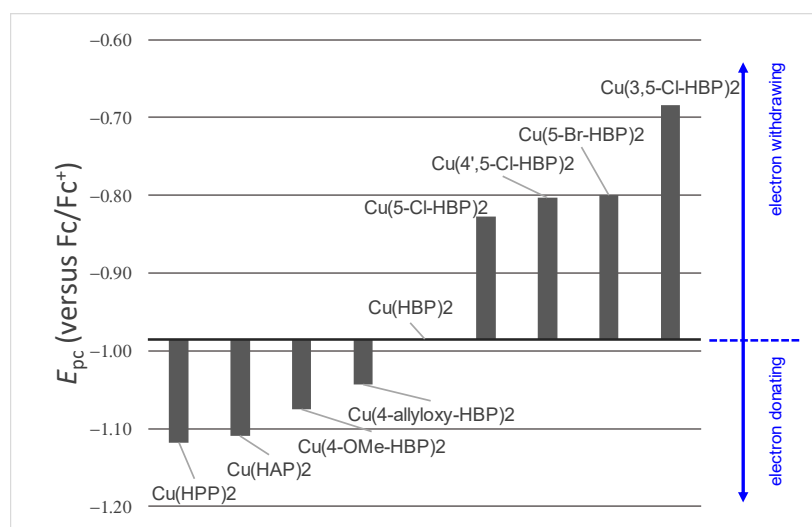


Figure 2. Reduction potential of copper-2-hydroxyphenone complexes (10–19) containing electron-donating (OEt, OCH₃) and electron withdrawing (Cl, Br) groups, relative to the copper-2-hydroxybenzophenone containing unsubstituted 2-hydroxybenzophenone (14). Data were obtained at a scan rate of 0.100 V s^{-1} in dimethyl sulfoxide as solvent from the related research article [8].

2.1. Benzophenones (1–9)

Reports on the reduction of benzophenone in non-aqueous solvents [9,10,40] indicate that the reduction occurs in two successive one-electron steps [41,42]. Cyclic voltammograms of the benzophenones (1–8), obtained in dimethylformamide as solvent, showing the first reduction step, are given in Figures 3–10. In Figure 11, cyclic voltammograms of the benzophenone (9), showing both reduction steps, are given. The first reduction peak on the cyclic voltammograms provides the energy needed (in volt) to reduce benzophenone and to re-oxidise the reduced benzophenone radical, namely the data related to the

benzophenone/[benzophenone^{•-}] redox process. The second irreversible one-electron reduction step is reported to correspond to the formation of an unstable benzhydrol dianion Bzph²⁻ [12,43,44]. Data obtained from the cyclic voltammograms are given in Tables 1–9, while the raw current-voltage values are provided in the supplementary information. The cyclic voltammograms and data presented provide additional electrochemical data to the reduction potential at the 0.10 V s⁻¹ scan rate, provided in the related research article [7]. The additional data illustrate that the observed electrochemical behaviour at 0.100 V s⁻¹ does not change at higher scan rates and that the reduction process is diffusion controlled.

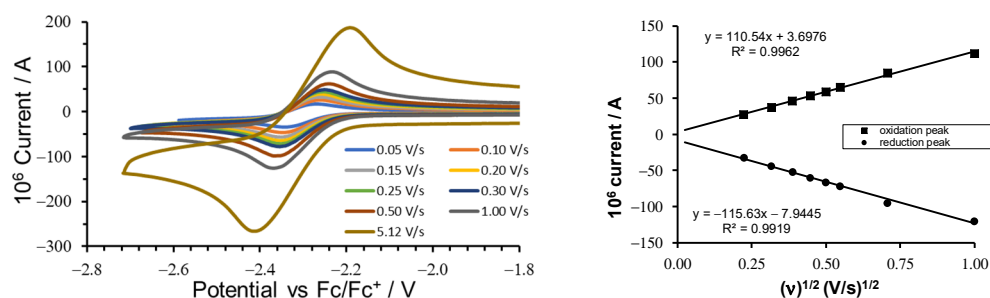


Figure 3. (Left) Cyclic voltammograms of ca 0.002 mol dm⁻³ 2-methylbenzophenone, 2-Me-bz (1) in dimethylformamide as solvent, 0.100 mol dm⁻³ TBAPF₆ as supporting electrolyte, reported versus Fc/Fc⁺. Scan rates are indicated. (Right) Linear relationship between the peak current (i_p) and the square root of the scan rate ($v^{1/2}$), as predicted by the Randles–Ševčík equation, for the oxidation (top graph) and reduction peak (bottom graph). (CV at 0.100 V s⁻¹ from related research article [7]).

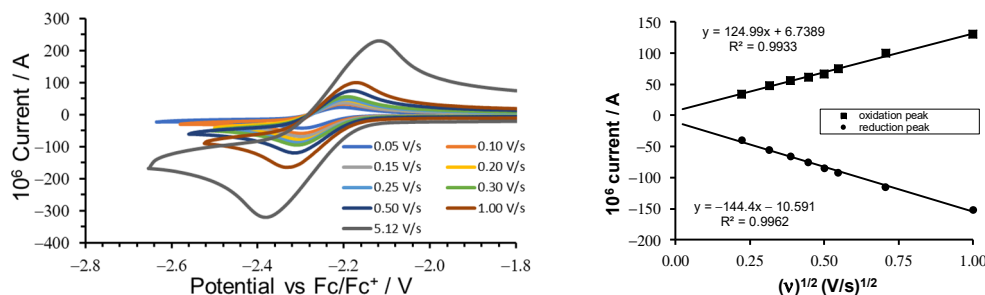


Figure 4. (Left) Cyclic voltammograms of ca 0.002 mol dm⁻³ 3-methylbenzophenone, 3-Me-bz (2) in dimethylformamide as solvent, 0.100 mol dm⁻³ TBAPF₆ as supporting electrolyte, reported versus Fc/Fc⁺. Scan rates are indicated. (Right) Linear relationship between the peak current (i_p) and the square root of the scan rate ($v^{1/2}$), as predicted by the Randles–Ševčík equation, for the oxidation (top graph) and reduction peak (bottom graph). (CV at 0.100 V s⁻¹ from related research article [7]).

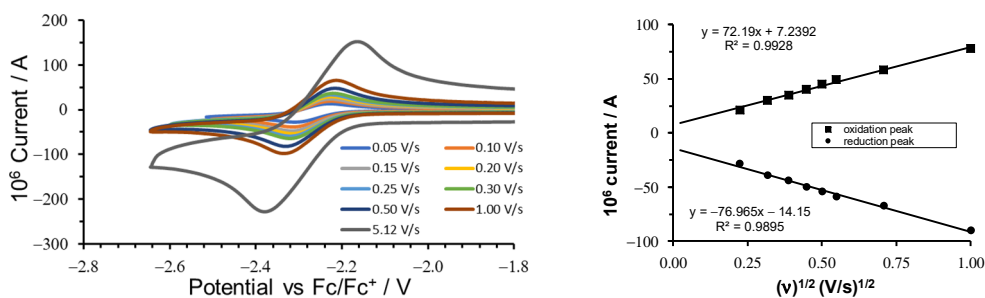


Figure 5. (Left) Cyclic voltammograms of ca 0.002 mol dm⁻³ 4-methylbenzophenone, 4-Me-bz (3) in dimethylformamide as solvent, 0.100 mol dm⁻³ TBAPF₆ as supporting electrolyte, reported versus Fc/Fc⁺. Scan rates are indicated. (Right) Linear relationship between the peak current (i_p) and the square root of the scan rate ($v^{1/2}$), as predicted by the Randles–Ševčík equation, for the oxidation (top graph) and reduction peak (bottom graph). (CV at 0.100 V s⁻¹ from related research article [7]).

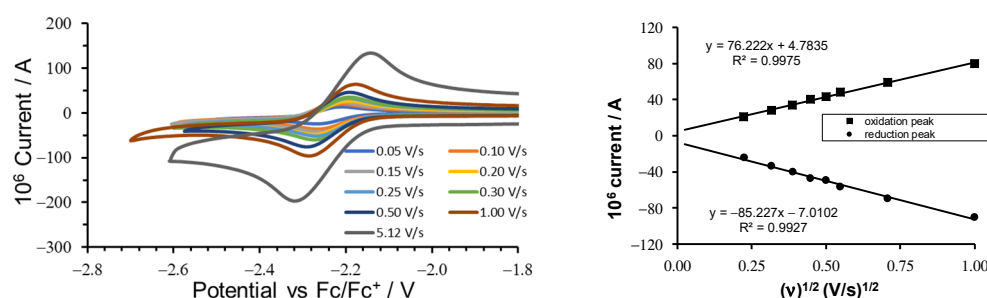


Figure 6. (Left) Cyclic voltammograms of ca 0.002 mol dm⁻³ 4-methoxybenzophenone, 4-OMe-bz (4) in dimethylformamide as solvent, 0.100 mol dm⁻³ TBAPF₆ as supporting electrolyte, reported versus Fc/Fc⁺. Scan rates are indicated. (Right) Linear relationship between the peak current (i_p) and the square root of the scan rate ($v^{1/2}$), as predicted by the Randles–Ševčík equation, for the oxidation (top graph) and reduction peak (bottom graph). (CV at 0.100 Vs⁻¹ from related research article [7]).

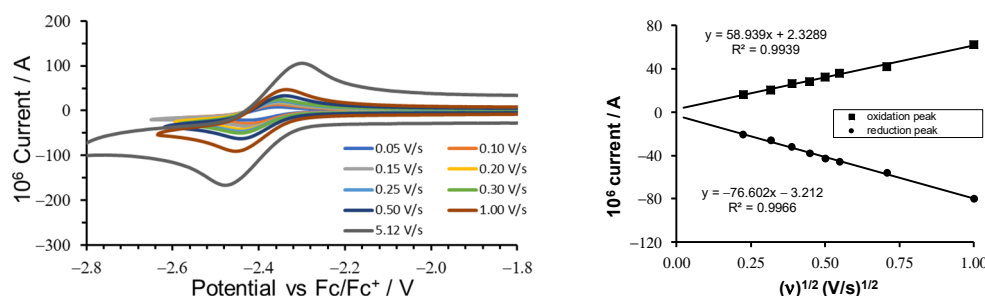


Figure 7. (Left) Cyclic voltammograms of ca 0.002 mol dm⁻³ 4,4'-dimethoxybenzophenone, 4,4'-OMe-bz (5) in dimethylformamide as solvent, 0.100 mol dm⁻³ TBAPF₆ as supporting electrolyte, reported versus Fc/Fc⁺. Scan rates are indicated. (Right) Linear relationship between the peak current (i_p) and the square root of the scan rate ($v^{1/2}$), as predicted by the Randles–Ševčík equation, for the oxidation (top graph) and reduction peak (bottom graph). (CV at 0.100 Vs⁻¹ from related research article [7]).

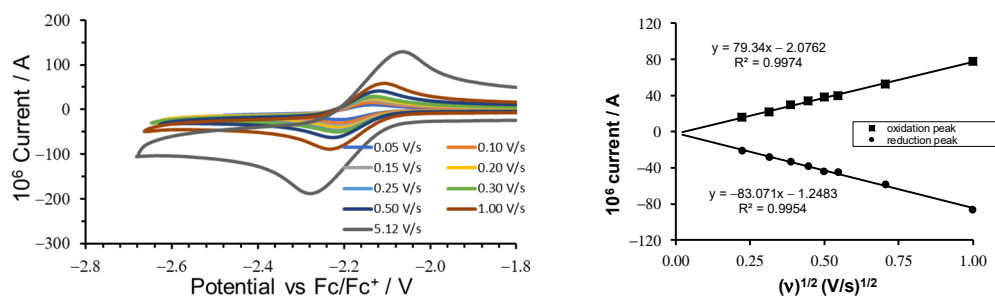


Figure 8. (Left) Cyclic voltammograms of ca 0.002 mol dm⁻³ 2-amino-5-chlorobenzophenone, 2-NH₂,5-Cl-bz (6) in dimethylformamide as solvent, 0.100 mol dm⁻³ TBAPF₆ as supporting electrolyte, reported versus Fc/Fc⁺. Scan rates are indicated. (Right) Linear relationship between the peak current (i_p) and the square root of the scan rate ($v^{1/2}$), as predicted by the Randles–Ševčík equation, for the oxidation (top graph) and reduction peak (bottom graph). (CV at 0.100 Vs⁻¹ from related research article [7]).

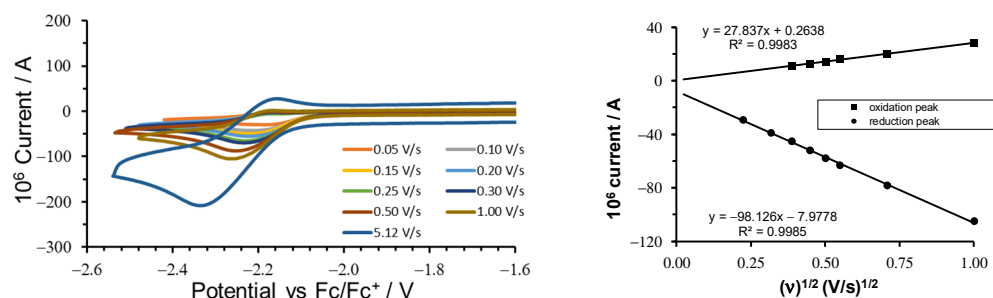


Figure 9. (Left) Cyclic voltammograms of ca 0.002 mol dm⁻³ 2-chlorobenzophenone, 2-Cl-bz (7) in dimethylformamide as solvent, 0.100 mol dm⁻³ TBAPF₆ as supporting electrolyte, reported versus Fc/Fc⁺. Scan rates are indicated. (Right) Linear relationship between the peak current (i_p) and the square root of the scan rate ($v^{1/2}$), for the second reduction peak, as predicted by the Randles–Ševčík equation for and reduction peak. (CV at 0.100 Vs⁻¹ from related research article [7]).

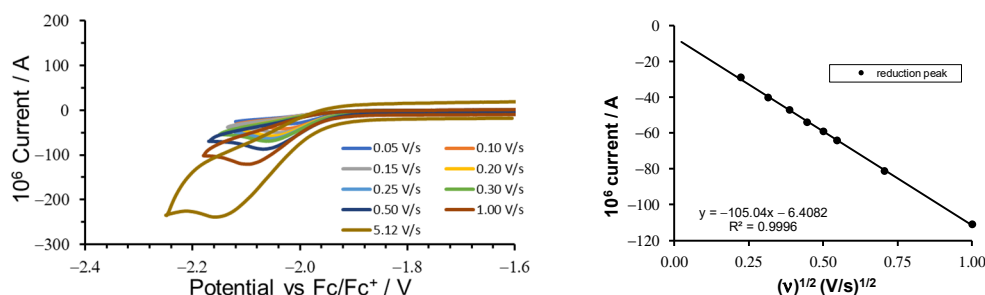


Figure 10. (Left) Cyclic voltammograms of ca 0.002 mol dm⁻³ 4-(Bromomethyl)benzophenone 4-CH₂Br-bz (8) in dimethylformamide as solvent, 0.100 mol dm⁻³ TBAPF₆ as supporting electrolyte reported versus Fc/Fc⁺. Scan rates are indicated. (Right) Linear relationship between the peak current (i_p) and the square root of the scan rate ($v^{1/2}$), for the second reduction peak, as predicted by the Randles–Ševčík equation for and reduction peak. (CV at 0.100 Vs⁻¹ from related research article [7]).

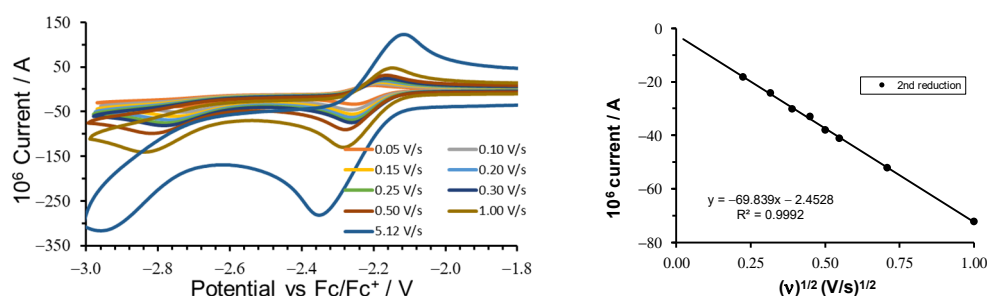


Figure 11. (Left) Cyclic voltammograms of ca 0.002 mol dm⁻³ benzophenone bz (10) in dimethylformamide as solvent, 0.100 mol dm⁻³ TBAPF₆ as supporting electrolyte, reported versus Fc/Fc⁺. Scan rates are indicated. (CV at 0.01 Vs⁻¹ from related research article [7]). (Right) Linear relationship between the peak current (i_p) and the square root of the scan rate ($v^{1/2}$), for the second reduction peak, as predicted by the Randles–Ševčík equation for and reduction peak. (CV at 0.100 Vs⁻¹ from related research article [7]). Linear relationship between the peak current (i_p) and the square root of the scan rate ($v^{1/2}$), for the first reduction peak, is available in the related research article [7].

Table 1. Electrochemical data obtained from the cyclic voltammograms of ca 0.002 mol dm⁻³ 2-methylbenzophenone, 2-Me-bz (**1**) in dimethylformamide as solvent, 0.100 mol dm⁻³ TBAPF₆ as supporting electrolyte, reported versus Fc/Fc⁺, at indicated scan rates ν (Vs⁻¹). (Potential data of 0.100 Vs⁻¹ from related research article [7]).

ν (Vs ⁻¹)	E_{pc} (V)	E_{pa} (V)	$E_{1/2}$ (V)	ΔE (V)	$10^6 i_{pc}$ (A)	i_{pa}/i_{pc}
0.05	-2.342	-2.269	-2.306	0.073	32	0.875
0.10	-2.350	-2.260	-2.305	0.090	44	0.841
0.15	-2.350	-2.260	-2.305	0.090	52	0.885
0.20	-2.350	-2.260	-2.305	0.090	60	0.900
0.25	-2.353	-2.258	-2.306	0.095	66	0.894
0.30	-2.356	-2.252	-2.304	0.104	72	0.903
0.50	-2.362	-2.244	-2.303	0.118	95	0.895
1.00	-2.366	-2.241	-2.304	0.125	120	0.933
5.12	-2.414	-2.195	-2.305	0.219	238	0.916

Table 2. Electrochemical data obtained from the cyclic voltammograms of ca 0.002 mol dm⁻³ 3-methylbenzophenone, 3-Me-bz (**2**) in dimethylformamide as solvent, 0.100 mol dm⁻³ TBAPF₆ as supporting electrolyte, reported versus Fc/Fc⁺, at indicated scan rates ν (Vs⁻¹). (Potential data of 0.100 Vs⁻¹ from related research article [7]).

ν (Vs ⁻¹)	E_{pc} (V)	E_{pa} (V)	$E_{1/2}$ (V)	ΔE (V)	$10^6 i_{pc}$ (A)	i_{pa}/i_{pc}
0.05	-2.291	-2.207	-2.249	0.084	40	0.850
0.10	-2.299	-2.200	-2.250	0.099	56	0.857
0.15	-2.300	-2.200	-2.250	0.100	66	0.848
0.20	-2.300	-2.200	-2.250	0.100	75	0.813
0.25	-2.305	-2.193	-2.249	0.112	85	0.776
0.30	-2.307	-2.193	-2.250	0.114	92	0.815
0.50	-2.317	-2.178	-2.248	0.139	115	0.870
1.00	-2.330	-2.170	-2.250	0.160	152	0.855
5.12	-2.381	-2.118	-2.250	0.263	298	0.879

Table 3. Electrochemical data obtained from the cyclic voltammograms of ca 0.002 mol dm⁻³ 4-methylbenzophenone, 4-Me-bz (**3**) in dimethylformamide as solvent, 0.100 mol dm⁻³ TBAPF₆ as supporting electrolyte, reported versus Fc/Fc⁺, at indicated scan rates ν (Vs⁻¹). (Potential data of 0.100 Vs⁻¹ from related research article [7]).

ν (Vs ⁻¹)	E_{pc} (V)	E_{pa} (V)	$E_{1/2}$ (V)	ΔE (V)	$10^6 i_{pc}$ (A)	i_{pa}/i_{pc}
0.05	-2.309	-2.233	-2.271	0.076	28	0.750
0.10	-2.320	-2.229	-2.275	0.091	39	0.769
0.15	-2.320	-2.226	-2.273	0.094	44	0.795
0.20	-2.320	-2.226	-2.273	0.094	50	0.800
0.25	-2.323	-2.223	-2.273	0.100	54	0.833
0.30	-2.324	-2.221	-2.273	0.103	59	0.831
0.50	-2.327	-2.219	-2.273	0.108	67	0.866
1.00	-2.335	-2.215	-2.275	0.120	90	0.867
5.12	-2.379	-2.164	-2.272	0.215	200	0.860

Table 4. Electrochemical data obtained from the cyclic voltammograms of ca 0.002 mol dm⁻³ 4-methoxybenzophenone, 4-Ome-bz (**4**) in dimethylformamide as solvent, 0.100 mol dm⁻³ TBAPF₆ as supporting electrolyte, reported versus Fc/Fc⁺, at indicated scan rates ν (Vs⁻¹). (Potential data of 0.100 Vs⁻¹ from related research article [7]).

ν (Vs ⁻¹)	E_{pc} (V)	E_{pa} (V)	$E_{1/2}$ (V)	ΔE (V)	$10^6 i_{pc}$ (A)	i_{pa}/i_{pc}
0.05	-2.269	-2.209	-2.239	0.060	24	0.875
0.10	-2.266	-2.206	-2.236	0.060	33	0.848
0.15	-2.266	-2.206	-2.236	0.060	40	0.850
0.20	-2.272	-2.196	-2.234	0.076	47	0.851
0.25	-2.272	-2.196	-2.234	0.076	49	0.878
0.30	-2.270	-2.194	-2.232	0.076	56	0.857
0.50	-2.287	-2.189	-2.238	0.098	69	0.855
1.00	-2.284	-2.182	-2.233	0.102	90	0.889
5.12	-2.320	-2.146	-2.233	0.174	166	0.916

Table 5. Electrochemical data obtained from the cyclic voltammograms of ca 0.002 mol dm⁻³ 4,4'-dimethoxybenzophenone, 4,4'-Ome-bz (**5**) in dimethylformamide as solvent, 0.100 mol dm⁻³ TBAPF₆ as supporting electrolyte, reported versus Fc/Fc⁺, at indicated scan rates ν (Vs⁻¹). (Potential data of 0.100 Vs⁻¹ from related research article [7]).

ν (Vs ⁻¹)	E_{pc} (V)	E_{pa} (V)	$E_{1/2}$ (V)	ΔE (V)	$10^6 i_{pc}$ (A)	i_{pa}/i_{pc}
0.05	-2.425	-2.356	-2.391	0.069	21	0.762
0.10	-2.425	-2.356	-2.391	0.069	26	0.769
0.15	-2.425	-2.356	-2.391	0.069	32	0.813
0.20	-2.433	-2.356	-2.395	0.077	38	0.737
0.25	-2.438	-2.354	-2.396	0.084	43	0.744
0.30	-2.440	-2.352	-2.396	0.088	46	0.783
0.50	-2.440	-2.336	-2.388	0.104	56	0.750
1.00	-2.447	-2.339	-2.393	0.108	80	0.775
5.00	-2.475	-2.301	-2.388	0.174	138	0.768

Table 6. Electrochemical data obtained from the cyclic voltammograms of ca 0.002 mol dm⁻³ 2-amino-5-chlorobenzophenone, 2-NH₂,5-Cl-bz (**6**) in dimethylformamide as solvent, 0.100 mol dm⁻³ TBAPF₆ as supporting electrolyte, reported versus Fc/Fc⁺, at indicated scan rates ν (Vs⁻¹). (Potential data of 0.100 Vs⁻¹ from related research article [7]).

ν (Vs ⁻¹)	E_{pc} (V)	E_{pa} (V)	$E_{1/2}$ (V)	ΔE (V)	$10^6 i_{pc}$ (A)	i_{pa}/i_{pc}
0.05	-2.204	-2.140	-2.172	0.064	21	0.76
0.10	-2.213	-2.135	-2.174	0.078	28	0.79
0.15	-2.207	-2.138	-2.173	0.069	33	0.91
0.20	-2.211	-2.131	-2.171	0.080	38	0.89
0.25	-2.216	-2.126	-2.171	0.090	44	0.86
0.30	-2.214	-2.134	-2.174	0.080	45	0.89
0.50	-2.228	-2.118	-2.173	0.110	58	0.91
1.00	-2.236	-2.106	-2.171	0.130	86	0.91
5.12	-2.278	-2.064	-2.171	0.214	164	0.91

Table 7. Electrochemical data obtained from the cyclic voltammograms of ca 0.002 mol dm⁻³ 2-chlorobenzophenone, 2-Cl-bz (7) in dimethylformamide as solvent, 0.100 mol dm⁻³ TBAPF₆ as supporting electrolyte, reported versus Fc/Fc⁺, at indicated scan rates ν (Vs⁻¹). (Potential data of 0.100 Vs⁻¹ from related research article [7]).

ν (Vs ⁻¹)	E_{pc} (V)	E_{pa} (V)	$E_{1/2}$ (V)	ΔE (V)	$10^6 i_{pc}$ (A)	i_{pa}/i_{pc}
0.05	-2.200	-	-	-	29	-
0.10	-2.217	-	-	-	39	-
0.15	-2.223	-2.166	-2.195	0.057	45	0.244
0.20	-2.224	-2.166	-2.195	0.058	52	0.240
0.25	-2.225	-2.166	-2.196	0.059	58	0.241
0.30	-2.231	-2.165	-2.198	0.066	63	0.254
0.50	-2.254	-2.164	-2.209	0.090	78	0.256
1.00	-2.257	-2.163	-2.210	0.094	105	0.267
5.12	-2.332	-2.158	-2.245	0.174	180	0.361

Table 8. Electrochemical data obtained from the cyclic voltammograms of ca 0.002 mol dm⁻³ 4-(Bromomethyl)benzophenone 4-CH₂Br-bz (8) in dimethylformamide as solvent, 0.100 mol dm⁻³ TBAPF₆ as supporting electrolyte, reported versus Fc/Fc⁺, at indicated scan rates ν (Vs⁻¹). (Potential data of 0.100 Vs⁻¹ from related research article [7]).

ν (Vs ⁻¹)	E_{pc} (V)	$10^6 i_{pc}$ (A)
0.05	-2.023	29
0.10	-2.042	40
0.15	-2.043	47
0.20	-2.049	54
0.25	-2.053	59
0.30	-2.057	64
0.50	-2.062	81
1.00	-2.093	111
5.12	-2.154	222

Table 9. Electrochemical data obtained from the cyclic voltammograms of ca 0.002 mol dm⁻³ benzophenone bz (10) in dimethylformamide as solvent, 0.100 mol dm⁻³ TBAPF₆ as supporting electrolyte, reported versus Fc/Fc⁺, at indicated scan rates ν (Vs⁻¹). (Potential data of 0.100 Vs⁻¹ from related research article [7]).

Peak		1st					2nd	
ν (Vs ⁻¹)	E_{pc} (V)	E_{pa} (V)	$E_{1/2}$ (V)	ΔE (V)	$10^6 i_{pc}$ (A)	i_{pa}/i_{pc}	E_{pc} (V)	$10^6 i_{pc}$ (A)
0.05	-2.256	-2.192	-2.224	0.064	27	0.89	-2.725	18
0.10	-2.262	-2.185	-2.224	0.077	39	0.81	-2.748	24
0.15	-2.262	-2.184	-2.223	0.078	45	0.90	-2.75	30
0.20	-2.263	-2.184	-2.224	0.079	53	0.90	-2.767	33
0.25	-2.265	-2.180	-2.223	0.085	56	0.93	-2.777	38
0.30	-2.266	-2.175	-2.221	0.091	61	0.95	-2.780	41
0.50	-2.276	-2.169	-2.223	0.107	80	0.93	-2.818	52
1.00	-2.287	-2.159	-2.223	0.128	108	0.95	-2.838	72
5.12	-2.345	-2.105	-2.225	0.240	218	0.96	-2.932	150

2.2. Copper-2-Hydroxyphenone Complexes (10–19)

Cyclic voltammograms of the Cu(II) complexes (10–19) are given in Figures 12–21. Data obtained from the cyclic voltammograms are given in Tables 10–16 (values at scan rate 0.100 V/s from the related research article [8]).

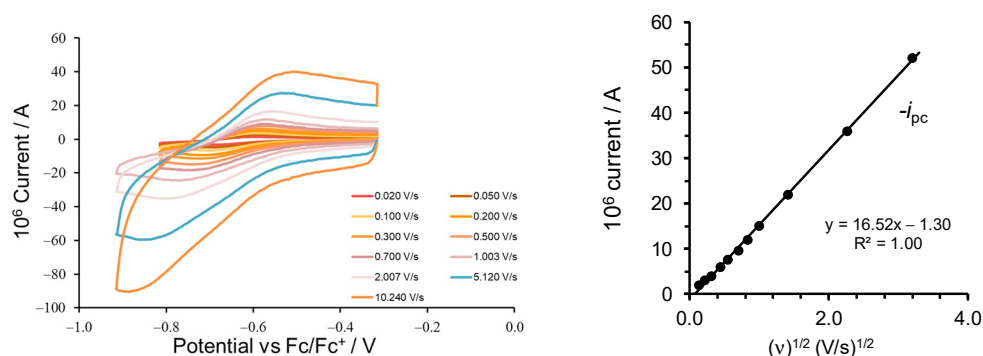


Figure 12. (Left) Cyclic voltammograms of ca 0.002 mol dm⁻³ Cu(3,5-Cl-HBP)₂ (10) in dimethyl sulfoxide as solvent, 0.100 mol dm⁻³ TBAPF₆ as supporting electrolyte, reported versus Fc/Fc⁺. Scan rates are indicated. (Right) Linear relationship between the peak reduction current ($-i_{pc}$) and the square root of the scan rate ($v^{1/2}$), as predicted by the Randles–Ševčík equation, for the reduction peak. CVs at scan rates 0.02–0.70 V/s from the related research article [8]. The peak oxidation current, i_{pa} , did not follow the Randles–Ševčík equation.

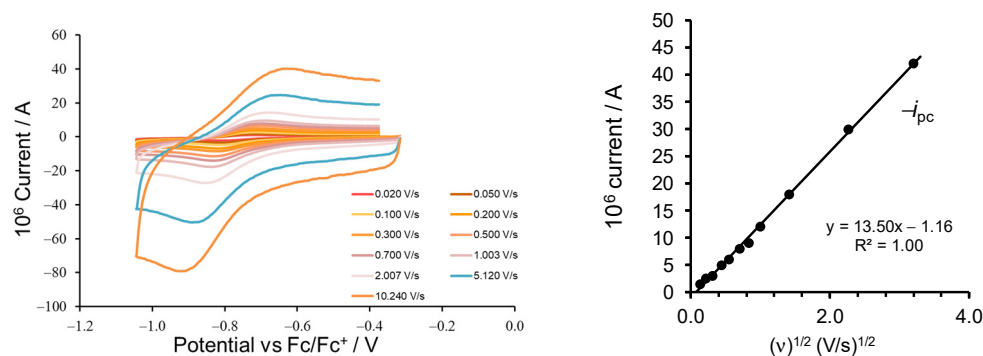


Figure 13. (Left) Cyclic voltammograms of ca 0.002 mol dm⁻³ Cu(5-Br-HBP)₂ (11) in dimethyl sulfoxide as solvent, 0.100 mol dm⁻³ TBAPF₆ as supporting electrolyte, reported versus Fc/Fc⁺. Scan rates are indicated. (Right) Linear relationship between the peak reduction current ($-i_{pc}$) and the square root of the scan rate ($v^{1/2}$), as predicted by the Randles–Ševčík equation, for the reduction peak. The peak oxidation current, i_{pa} , did not follow the Randles–Ševčík equation.

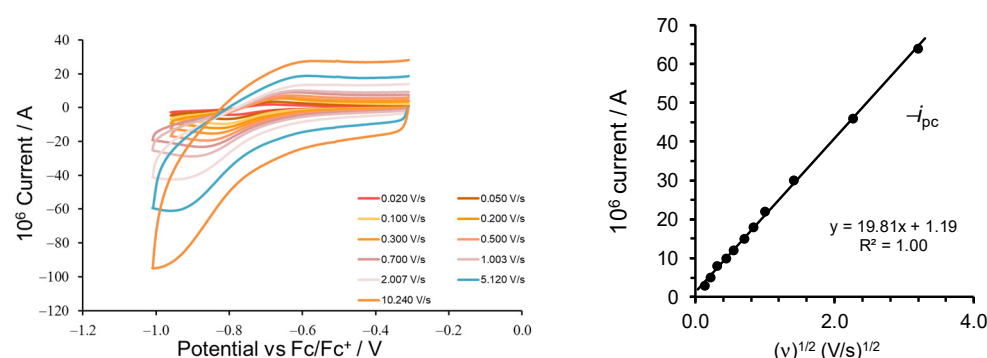


Figure 14. (Left) Cyclic voltammograms of ca 0.002 mol dm⁻³ Cu(4',5-Cl-HBP)₂ (12) in dimethyl sulfoxide as solvent, 0.100 mol dm⁻³ TBAPF₆ as supporting electrolyte, reported versus Fc/Fc⁺. Scan rates are indicated. (Right) Linear relationship between the peak reduction current ($-i_{pc}$) and the square root of the scan rate ($v^{1/2}$) (Randles–Ševčík equation), for the reduction peak.

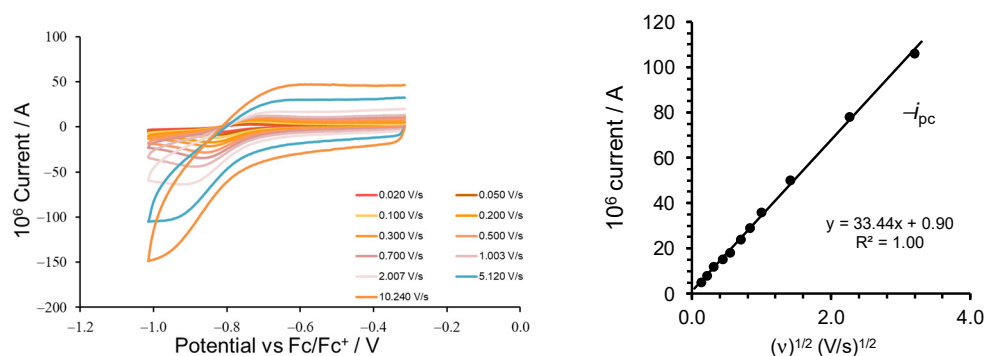


Figure 15. (Left) Cyclic voltammograms of ca 0.002 mol dm⁻³ Cu(5-Cl-HBP)₂ (13) in dimethyl sulfoxide as solvent, 0.100 mol dm⁻³ TBAPF₆ as supporting electrolyte, reported versus Fc/Fc⁺. Scan rates are indicated. (Right) Linear relationship between the peak reduction current ($-i_{pc}$) and the square root of the scan rate ($v^{1/2}$), as predicted by the Randles–Ševčík equation, for the reduction peak.

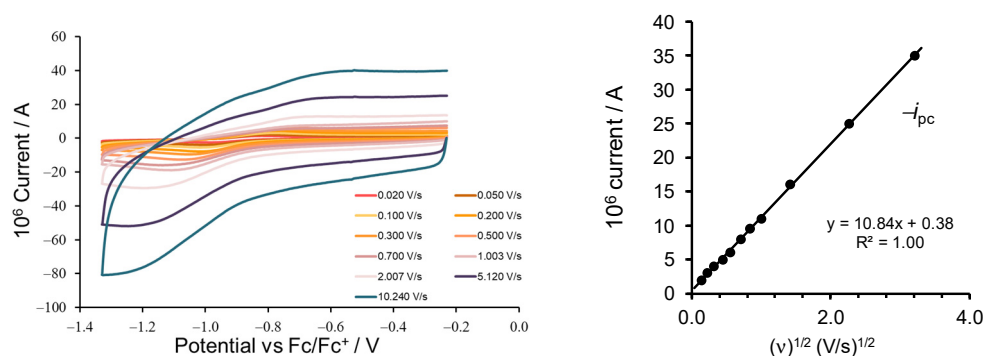


Figure 16. (Left) Cyclic voltammograms of ca 0.002 mol dm⁻³ Cu(HBP)₂ (14) in dimethyl sulfoxide as solvent, 0.100 mol dm⁻³ TBAPF₆ as supporting electrolyte, reported versus Fc/Fc⁺. Scan rates are indicated. (Right) Linear relationship between the peak reduction current ($-i_{pc}$) and the square root of the scan rate ($v^{1/2}$), as predicted by the Randles–Ševčík equation, for the reduction peak.

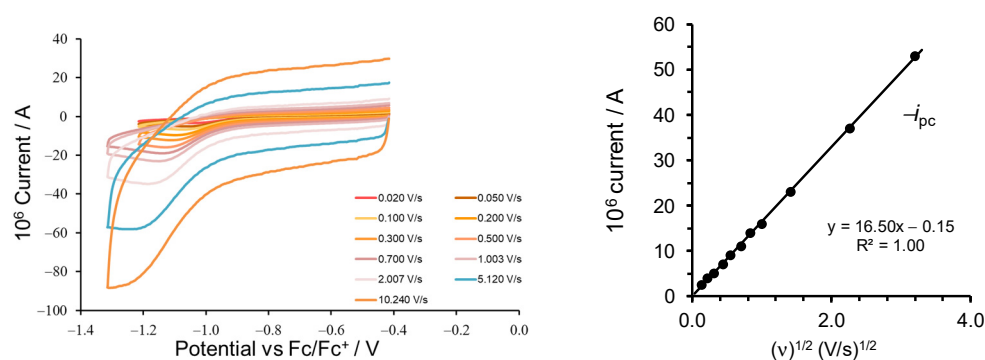


Figure 17. (Left) Cyclic voltammograms of ca 0.002 mol dm⁻³ Cu(4-allyloxy-HBP)₂ (15) in dimethyl sulfoxide as solvent, 0.100 mol dm⁻³ TBAPF₆ as supporting electrolyte, reported versus Fc/Fc⁺. Scan rates are indicated. (Right) Linear relationship between the peak reduction current ($-i_{pc}$) and the square root of the scan rate ($v^{1/2}$), as predicted by the Randles–Ševčík equation, for the reduction peak. CVs at scan rates 0.02–0.70 V/s from the related research article [8].

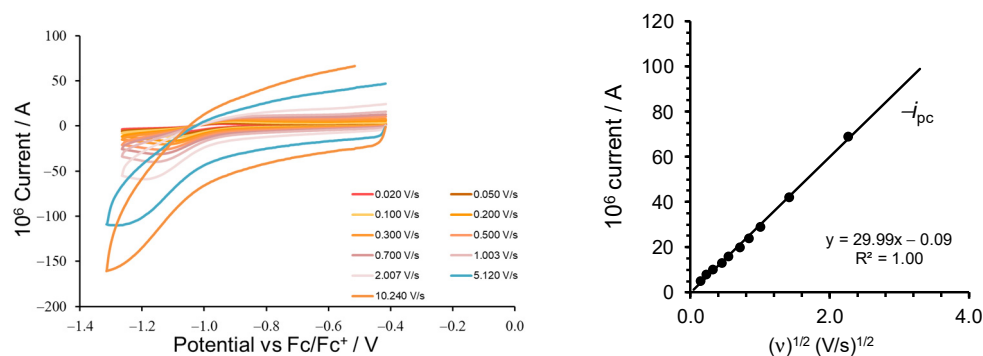


Figure 18. (Left) Cyclic voltammograms of ca 0.002 mol dm⁻³ Cu(4-OMe-HBP)₂ (16) in dimethyl sulfoxide as solvent, 0.100 mol dm⁻³ TBAPF₆ as supporting electrolyte, reported versus Fc/Fc⁺. Scan rates are indicated. (Right) Linear relationship between the peak reduction current ($-i_{pc}$) and the square root of the scan rate ($v^{1/2}$), as predicted by the Randles–Ševčík equation for the reduction peak.

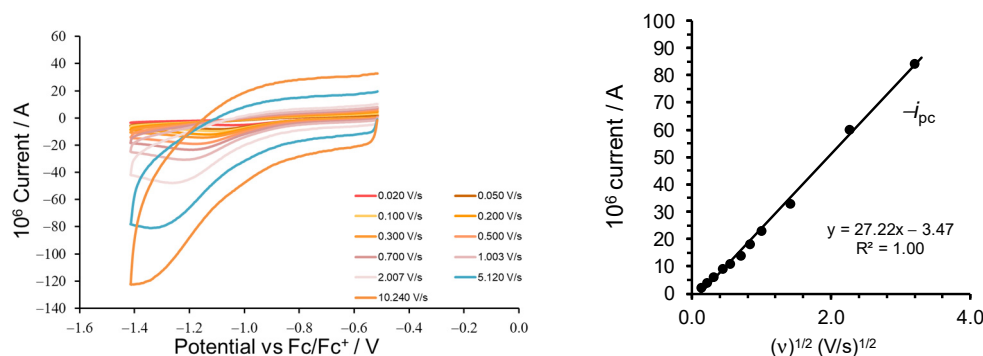


Figure 19. (Left) Cyclic voltammograms of ca 0.002 mol dm⁻³ Cu(HAP)₂ (17) in dimethyl sulfoxide as solvent, 0.100 mol dm⁻³ TBAPF₆ as supporting electrolyte, reported versus Fc/Fc⁺. Scan rates are indicated. (Right) Linear relationship between the peak reduction current ($-i_{pc}$) and the square root of the scan rate ($v^{1/2}$), as predicted by the Randles–Ševčík equation for the reduction peak.

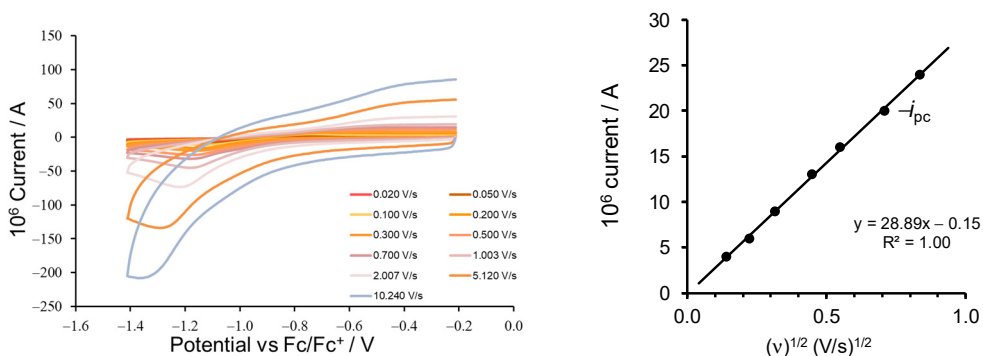


Figure 20. (Left) Cyclic voltammograms of ca 0.002 mol dm⁻³ Cu(HPP)₂ (18) in dimethyl sulfoxide as solvent, 0.100 mol dm⁻³ TBAPF₆ as supporting electrolyte, reported versus Fc/Fc⁺. Scan rates are indicated. (Right) Linear relationship between the peak reduction current ($-i_{pc}$) and the square root of the scan rate ($v^{1/2}$), as predicted by the Randles–Ševčík equation for the reduction peak.

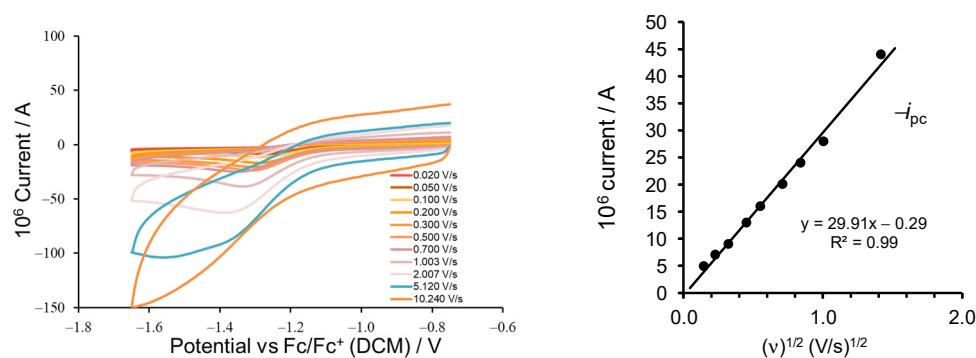


Figure 21. (Left) Cyclic voltammograms of ca 0.002 mol dm⁻³ Cu(4-Oct-HBP)₂ (**19**) in dichloromethane as solvent, 0.100 mol dm⁻³ TBAPF₆ as supporting electrolyte, reported versus Fc/Fc⁺. Scan rates are indicated. (Right) Linear relationship between the peak reduction current ($-i_{pc}$) and the square root of the scan rate ($v^{1/2}$), as predicted by the Randles-Sěvcik equation for the reduction peak.

Table 10. Electrochemical data obtained from the cyclic voltammograms of ca 0.002 mol dm⁻³ Cu(3,5-Cl-HBP)₂ (**10**) in dimethyl sulfoxide as solvent, 0.100 mol dm⁻³ TBAPF₆ as supporting electrolyte, reported versus Fc/Fc⁺, at indicated scan rates v (Vs⁻¹).

v (Vs ⁻¹)	E_{pc} (V)	E_{pa} (V)	$E_{1/2}$ (V)	ΔE (V)	$10^6 i_{pc}$ (A)	i_{pa}/i_{pc}
0.020	-0.695	-0.605	-0.650	0.090	2	0.500
0.050	-0.681	-0.600	-0.641	0.081	3	0.500
0.100	-0.684	-0.605	-0.645	0.079	4	0.500
0.200	-0.695	-0.592	-0.644	0.103	6	0.333
0.300	-0.700	-0.587	-0.644	0.113	8	0.333
0.500	-0.708	-0.571	-0.640	0.137	10	0.211
0.700	-0.714	-0.574	-0.644	0.140	12	0.125
1.000	-0.756	-0.548	-0.652	0.208	15	0.533
2.007	-0.778	-0.547	-0.663	0.231	22	0.318
5.120	-0.790	-0.578	-0.106	1.368	36	0.083
10.240	-0.859	-0.514	-0.687	0.345	52	-

Table 11. Electrochemical data obtained from the cyclic voltammograms of ca 0.002 mol dm⁻³ Cu(5-Br-HBP)₂ (**11**) in dimethyl sulfoxide as solvent, 0.100 mol dm⁻³ TBAPF₆ as supporting electrolyte, reported versus Fc/Fc⁺, at indicated scan rates v (Vs⁻¹). (Potential data of 0.100 Vs⁻¹ from related research article).

v (Vs ⁻¹)	E_{pc} (V)	E_{pa} (V)	$E_{1/2}$ (V)	ΔE (V)	$10^6 i_{pc}$ (A)	i_{pa}/i_{pc}
0.020	-0.787	-0.728	-0.758	0.059	2	0.667
0.050	-0.796	-0.728	-0.762	0.068	3	0.800
0.100	-0.800	-0.728	-0.764	0.072	3	0.667
0.200	-0.802	-0.720	-0.761	0.082	5	0.600
0.300	-0.811	-0.715	-0.763	0.096	6	0.667
0.500	-0.818	-0.711	-0.765	0.107	8	0.625
0.700	-0.818	-0.706	-0.762	0.112	9	0.556
1.000	-0.830	-0.698	-0.764	0.132	12	0.500
2.007	-0.851	-0.676	-0.764	0.175	18	-
5.120	-0.886	-0.643	-0.765	0.243	30	-
10.240	-0.916	-0.626	-0.771	0.290	42	-

Table 12. E Electrochemical data obtained from the cyclic voltammograms of ca 0.002 mol dm⁻³ Cu(4',5-Cl-HBP)₂ (**12**) in dimethyl sulfoxide as solvent, 0.100 mol dm⁻³ TBAPF₆ as supporting electrolyte, reported versus Fc/Fc⁺, at indicated scan rates ν (Vs⁻¹).

ν (Vs ⁻¹)	E_{pc} (V)	E_{pa} (V)	$E_{1/2}$ (V)	ΔE (V)	$10^6 i_{pc}$ (A)	i_{pa}/i_{pc}
0.020	-0.778	-0.685	-0.732	0.093	3	0.667
0.050	-0.791	-0.680	-0.736	0.111	5	0.600
0.100	-0.803	-0.667	-0.735	0.136	8	0.625
0.200	-0.809	-0.662	-0.736	0.147	10	0.300
0.300	-0.827	-0.658	-0.743	0.169	12	0.250
0.500	-0.849	-0.671	-0.760	0.178	15	0.133
0.700	-0.853	-0.645	-0.749	0.208	18	0.111
1.000	-0.883	-0.631	-0.757	0.252	22	0.045
2.007	-0.906	-0.618	-0.762	0.288	30	-
5.120	-0.913	-0.620	-0.767	0.293	46	-
10.240	-0.940	-0.600	-0.770	0.340	64	-

Table 13. Electrochemical data obtained from the cyclic voltammograms of ca 0.002 mol dm⁻³ Cu(5-Cl-HBP)₂ (**13**) in dimethyl sulfoxide as solvent, 0.100 mol dm⁻³ TBAPF₆ as supporting electrolyte, reported versus Fc/Fc⁺, at indicated scan rates ν (Vs⁻¹). (Potential data of 0.100 Vs⁻¹ from related research article).

ν (Vs ⁻¹)	E_{pc} (V)	E_{pa} (V)	$E_{1/2}$ (V)	ΔE (V)	$10^6 i_{pc}$ (A)	i_{pa}/i_{pc}
0.020	-0.821	-0.73	-0.776	0.091	5	0.800
0.050	-0.827	-0.72	-0.774	0.107	8	0.625
0.100	-0.827	-0.715	-0.771	0.112	12	0.500
0.200	-0.831	-0.714	-0.773	0.117	15	0.533
0.300	-0.841	-0.714	-0.778	0.127	18	0.444
0.500	-0.846	-0.714	-0.780	0.132	24	0.333
0.700	-0.861	-0.714	-0.788	0.147	29	0.276
1.000	-0.877	-0.711	-0.794	0.166	36	0.222
2.007	-0.909	-0.693	-0.801	0.216	50	-
5.120	-0.941	-0.658	-0.800	0.283	78	-
10.240	-0.950	-0.635	-0.793	0.315	106	-

Table 14. Electrochemical data obtained from the cyclic voltammograms of ca 0.002 mol dm⁻³ Cu(HBP)₂ (**14**) in dimethyl sulfoxide as solvent, 0.100 mol dm⁻³ TBAPF₆ as supporting electrolyte, reported versus Fc/Fc⁺, at indicated scan rates ν (Vs⁻¹). (Potential data of 0.100 Vs⁻¹ from related research article).

ν (Vs ⁻¹)	E_{pc} (V)	E_{pa} (V)	$E_{1/2}$ (V)	ΔE (V)	$10^6 i_{pc}$ (A)	i_{pa}/i_{pc}
0.020	-0.979	-0.839	-0.909	0.140	2	0.750
0.050	-0.979	-0.817	-0.898	0.162	3	0.500
0.100	-0.985	-0.825	-0.905	0.160	4	0.500
0.200	-0.977	-0.822	-0.900	0.155	5	0.600
0.300	-1.014	-0.764	-0.889	0.250	6	0.500
0.500	-1.043	-0.751	-0.897	0.292	8	0.188
0.700	-1.087	-0.777	-0.932	0.310	9.5	-
1.000	-1.074	-0.728	-0.901	0.346	11	-
2.007	-1.137	-0.693	-0.915	0.444	16	-
5.120	-1.179	-0.675	-0.927	0.504	25	-
10.240	-1.150	-0.631	-0.891	0.519	35	-

Table 15. Electrochemical data obtained from the cyclic voltammograms of ca 0.002 mol dm⁻³ Cu(4-OMe-HBP)₂ (**15**) in dimethyl sulfoxide as solvent, 0.100 mol dm⁻³ TBAPF₆ as supporting electrolyte, reported versus Fc/Fc⁺, at indicated scan rates ν (Vs⁻¹). (Potential data of 0.100 Vs⁻¹ from related research article).

ν (Vs ⁻¹)	E_{pc} (V)	E_{pa} (V)	$E_{1/2}$ (V)	ΔE (V)	$10^6 i_{pc}$ (A)	i_{pa}/i_{pc}
0.020	-1.052	-0.963	-1.008	0.089	5	0.60
0.050	-1.065	-0.958	-1.012	0.107	8	0.63
0.100	-1.075	-0.941	-1.008	0.134	10	0.50
0.200	-1.087	-0.932	-1.010	0.155	13	0.38
0.300	-1.105	-0.914	-1.010	0.191	16	0.25
0.500	-1.123	-0.901	-1.012	0.222	20	0.10
0.700	-1.131	-0.901	-1.016	0.230	24	–
1.000	-1.140	–	-0.570	1.140	29	–
2.007	-1.180	–	-0.590	1.180	42	–
5.120	-1.226	–	-0.613	1.226	69	–
10.240	-1.307	–	-0.654	1.307	–	–

Table 16. Electrochemical data obtained from the cyclic voltammograms of ca 0.002 mol dm⁻³ Cu(4-allyloxy-HBP)₂ (**16**), Cu(HAP)₂ (**17**), Cu(HPP)₂ (**18**), and Cu(4-Oct-HBP)₂ (**19**) in the indicated solvent (dimethyl sulfoxide DMSO or dichloromethane DCM), 0.100 mol dm⁻³ TBAPF₆ as supporting electrolyte, reported versus Fc/Fc⁺, at indicated scan rates ν (Vs⁻¹). (Potential data of 0.100 Vs⁻¹ from related research article).

ν (Vs ⁻¹)	Cu(4-Allyloxy-HBP) ₂ (16) in DMSO		Cu(HAP) ₂ (17) in DMSO		Cu(HPP) ₂ (18) in DMSO		Cu(4-Oct-HBP) ₂ (19) in DCM	
	E_{pc} (V)	$10^6 i_{pc}$ (A)	E_{pc} (V)	$10^6 i_{pc}$ (A)	E_{pc} (V)	$10^6 i_{pc}$ (A)	E_{pc} (V)	$10^6 i_{pc}$ (A)
0.020	-1.101	2.5	-1.013	2	-1.044	4	-1.233	5
0.050	-1.036	4	-1.063	4	-1.108	6	-1.251	7
0.100	-1.043	5	-1.109	6	-1.118	9	-1.260	9
0.200	-1.065	7	-1.111	9	-1.123	13	-1.277	13
0.300	-1.109	9	-1.127	11	-1.132	16	-1.282	16
0.500	-1.118	11	-1.149	14	-1.154	20	-1.293	20
0.700	-1.123	14	-1.167	18	-1.158	24	-1.327	24
1.000	-1.127	16	-1.190	23	-1.174	35	-1.328	28
2.007	-1.170	23	-1.234	33	-1.213	55	-1.376	44
5.120	-1.202	37	-1.308	60	-1.272	100	-1.494	104
10.240	-1.241	53	-1.306	84	-1.320	155	-1.233	–

3. Methods

The benzophenone ligands were obtained from Sigma Aldrich and used as is. The copper-2-hydroxyphenone complexes **10–19** were synthesised, cleaned, and characterised as described in the related research article [8]. The CVs were obtained using a BAS100B Electrochemical Analyzer connected to a desktop computer (with BAS100W version 2.3 software) under similar conditions as those described in the related research articles [7,8] and our previous work [45]. The obtained current-voltage values of the CVs were exported as CSV files to be opened in Excel to visualise the results. The BAS100W version 2.3 software also provides the peak current i_p and peak current voltage E_p of the observed redox peaks. To obtain i_p and E_p data from a CV is well-described in the literature [46,47]. Figure 22 shows the determination of i_p and E_p from a CV of 2-NH₂,5-Cl-bz (**6**).

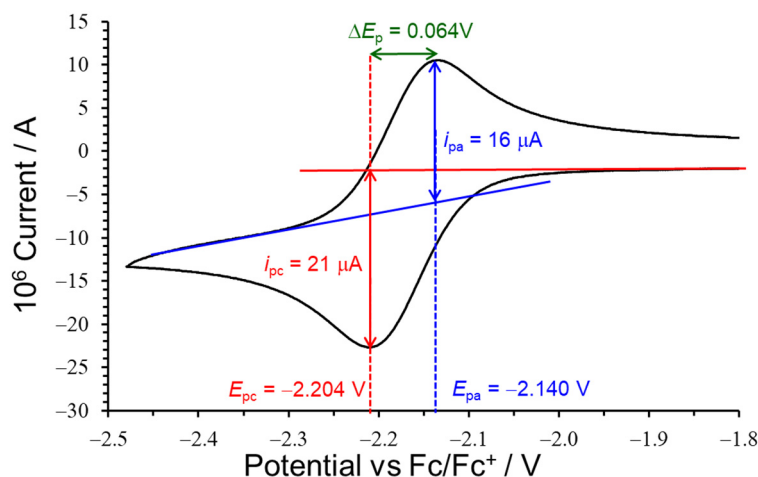


Figure 22. Illustration of how to obtain i_p and E_p data from a CV using CV of the reduction of ca $0.002 \text{ mol dm}^{-3}$ 2-amino-5-chlorobenzophenone, 2-NH₂,5-Cl-bz (**6**) in dimethylformamide as solvent, $0.100 \text{ mol dm}^{-3}$ TBAPF₆ as supporting electrolyte, scan rate $\nu = 0.050 \text{ Vs}^{-1}$. E_{pa} = peak anodic potential, E_{pc} = peak cathodic potential, i_{pa} = anodic peak current, i_{pc} = cathodic peak current. Peak potential separation $\Delta E_p = E_{pa} - E_{pc}$ and half-wave potential $E_{1/2} = (E_{pa} - E_{pc})/2$.

Supplementary Materials: The following supporting information can be downloaded at: <https://www.mdpi.com/article/10.3390/data7120183/s1>, Excel files with current-voltage data

Author Contributions: Conceptualization, J.C.; methodology, J.C.; validation, J.C.; formal analysis, J.C. and E.C.; investigation, E.C.; resources, J.C. and E.H.G.L.; data curation, E.C.; writing—original draft preparation, E.C.; writing—review and editing, J.C. and E.H.G.L.; visualisation, J.C. and E.C.; supervision, J.C.; project administration, J.C.; funding acquisition, J.C. and E.H.G.L. All authors have read and agreed to the published version of the manuscript.

Funding: This research was funded by the South African National Research Foundation, grant numbers 129270 and 132504, and Central Research Fund of the University of the Free State, Bloemfontein. The APC was funded by the Open Access Publications Fund (OAPF) of the University of the Free State.

Institutional Review Board Statement: Not applicable.

Informed Consent Statement: Not applicable.

Data Availability Statement: Within the article and the Supplementary Material.

Conflicts of Interest: The authors declare no conflict of interest.

References

1. Wu, S.-B.; Long, C.; Kennelly, E.J. Structural Diversity and Bioactivities of Natural Benzophenones. *Nat. Prod. Rep.* **2014**, *31*, 1158–1174. [[CrossRef](#)] [[PubMed](#)]
2. Porosa, L.; Caschera, A.; Bedard, J.; Mocella, A.; Ronan, E.; Lough, A.J.; Wolfaardt, G.; Foucher, D.A. UV-Curable Contact Active Benzophenone Terminated Quaternary Ammonium Antimicrobials for Applications in Polymer Plastics and Related Devices. *ACS Appl. Mater. Interfaces* **2017**, *9*, 27491–27503. [[CrossRef](#)] [[PubMed](#)]
3. Cheng, L.; Shi, W. Synthesis and Photoinitiating Behavior of Benzophenone-Based Polymeric Photoinitiators Used for UV Curing Coatings. *Prog. Org. Coat.* **2011**, *71*, 355–361. [[CrossRef](#)]
4. Kim, S.; Choi, K. Occurrences, Toxicities, and Ecological Risks of Benzophenone-3, a Common Component of Organic Sunscreen Products: A Mini-Review. *Environ. Int.* **2014**, *70*, 143–157. [[CrossRef](#)] [[PubMed](#)]
5. Huo, Y.; Xing, X.; Zhang, C.; Wang, X.; Li, Y. An All Organic Redox Flow Battery with High Cell Voltage. *RSC Adv.* **2019**, *9*, 13128–13132. [[CrossRef](#)]
6. DiNardo, J.C.; Downs, C.A. Dermatological and Environmental Toxicological Impact of the Sunscreen Ingredient Oxybenzone/Benzophenone-3. *J. Cosmet. Dermatol.* **2018**, *17*, 15–19. [[CrossRef](#)]
7. Chiyindiko, E.; Conradie, J. An Electrochemical and Computational Chemistry Study of Substituted Benzophenones. *Electrochim. Acta* **2021**, *373*, 137894. [[CrossRef](#)]

8. Chiyindikio, E.; Langner, E.H.G.; Conradie, J. Electrochemical Behaviour of Copper(II) Complexes Containing 2-Hydroxyphenones. *Electrochim. Acta* **2022**, *424*, 140629. [[CrossRef](#)]
9. Tsierkezos, N.G. Investigation of the Electrochemical Reduction of Benzophenone in Aprotic Solvents Using the Method of Cyclic Voltammetry. *J. Solut. Chem.* **2007**, *36*, 1301–1310. [[CrossRef](#)]
10. Tsierkezos, N.G.; Ritter, U. Application of Electrochemical Impedance Spectroscopy for Characterisation of the Reduction of Benzophenone in Acetonitrile Solutions. *Phys. Chem. Liq.* **2011**, *49*, 729–742. [[CrossRef](#)]
11. Grimshaw, J.; Hamilton, R. Steric and Electronic Effects on the Redox Potentials of Benzophenone Radical Anions. *J. Electroanal. Chem. Interfacial Electrochem.* **1980**, *106*, 339–346. [[CrossRef](#)]
12. Degrand, C.; Prest, R.; Compagnon, P. Iodine Electrochemical Synthesis of (Phenylseleno)Benzophenones and (Phenyltelluro)Benzophenones by the SRN1 Mechanism, Using a Redox Catalyst. *J. Org. Chem.* **1987**, *52*, 5229–5233. [[CrossRef](#)]
13. Jensen, B.S.; Parker, V.D. Reversible Anion Radical–Dianion Redox Equilibria Involving Ions of Simple Aromatic Compounds. *J. Chem. Soc. Chem. Commun.* **1974**, *167*, 367–368. [[CrossRef](#)]
14. Fawcett, W.R.; Fedurco, M. Medium Effects in the Electroreduction of Benzophenone in Aprotic Solvents. *J. Phys. Chem.* **1993**, *97*, 7075–7080. [[CrossRef](#)]
15. Curphey, T.J.; Trivedi, L.D.; Layloff, T. Electrochemical Reductive Acylation of Benzophenone. *J. Org. Chem.* **1974**, *39*, 3831–3834. [[CrossRef](#)]
16. Isse, A.A.; Galia, A.; Belfiore, C.; Silvestri, G.; Gennaro, A. Electrochemical Reduction and Carboxylation of Halobenzophenones. *J. Electroanal. Chem.* **2002**, *526*, 41–52. [[CrossRef](#)]
17. Bewick, A.; Jones, V.W.; Kalaji, M. Spectroscopic and Electrochemical Properties of Substituted Benzophenones and Their Related Ketyls. *Electrochim. Acta* **1996**, *41*, 1961–1970. [[CrossRef](#)]
18. Chiyindikio, E.; Langner, E.H.G.; Conradie, J. Cyclic Voltammetry Data of 2-Hydroxybenzophenones and Related Molecules. *Chem. Data Collect.* **2022**, *40*, 100897. [[CrossRef](#)]
19. Chiyindikio, E.; Langner, E.H.G.; Conradie, J. Electrochemical Behaviour of 2-Hydroxybenzophenones and Related Molecules. *Results Chem.* **2022**, *4*, 100332. [[CrossRef](#)]
20. Adeniyi, A.A.; Ngake, T.L.; Conradie, J. Cyclic Voltammetric Study of 2-Hydroxybenzophenone (HBP) Derivatives and the Correspondent Change in the Orbital Energy Levels in Different Solvents. *Electroanalysis* **2020**, *32*, 2659–2668. [[CrossRef](#)]
21. Gonçalves, C.B.; Marinho, M.V.; Dias, D.F.; Dos Santos, M.H.; Martins, F.T.; Doriguetto, A.C. Synthesis, Characterization, and Structural Determination of Copper(II) Complexes with Alkyl Derivatives of Hydroxybenzophenones. *J. Coord. Chem.* **2017**, *70*, 898–913. [[CrossRef](#)]
22. Zianna, A.; Psomas, G.; Hatzidimitriou, A.; Lalia-Kantouri, M. Copper(II) Complexes of Salicylaldehydes and 2-Hydroxyphenones: Synthesis, Structure, Thermal Decomposition Study and Interaction with Calf-Thymus DNA and Albumins. *RSC Adv.* **2015**, *5*, 37495–37511. [[CrossRef](#)]
23. Mao, G.Z.; Nong, X.L.; Zhang, S.H. Bis(2-Methoxy-Phenolato-2O,O')Copper(II). *Acta Crystallogr. Sect. E Struct. Reports Online* **2009**, *65*, m1208. [[CrossRef](#)] [[PubMed](#)]
24. Chiyindikio, E.; Conradie, J. Redox Behaviour of Bis(β -Diketonato)Copper(II) Complexes. *J. Electroanal. Chem.* **2019**, *837*, 76–85. [[CrossRef](#)]
25. Chiyindikio, E.; Stuurman, N.N.F.; Langner, E.H.G.; Conradie, J. Electrochemical Behaviour of Bis(β -Diketonato)Copper(II) Complexes Containing γ -Substituted β -Diketones. *J. Electroanal. Chem.* **2020**, *860*, 113929. [[CrossRef](#)]
26. Nunes, P.; Nagy, N.V.; Alegria, E.C.B.A.; Pombeiro, A.J.L.; Correia, I. The Solvation and Electrochemical Behavior of Copper Acetylacetonate Complexes in Ionic Liquids. *J. Mol. Struct.* **2014**, *1060*, 142–149. [[CrossRef](#)]
27. Anderson, C.W.; Lung, K.R.; Nile, T.A. Electrochemistry of Homogeneous Catalysts: Correlation of the Electrochemistry and the Ziegler–Natta Catalytic Activity of Metal Acetylacetonate Complexes. *Inorg. Chim. Acta* **1984**, *85*, 33–36. [[CrossRef](#)]
28. Al-Anber, M.A. Electrochemical Behaviour and Electronic Absorption of the Metal β -Diketonates Complexes. *Am. J. Phys. Chem.* **2013**, *2*, 1. [[CrossRef](#)]
29. Conradie, J. Bis(Acetylacetonato)Copper(II)–Structural and Electronic Data of the Neutral, Oxidized and Reduced Forms. *Data Br.* **2019**, *26*, 104511. [[CrossRef](#)]
30. Kuhn, A.; von Eschwege, K.G.; Conradie, J. Electrochemical and Density Functional Theory Modeled Reduction of Enolized 1,3-Diketones. *Electrochim. Acta* **2011**, *56*, 6211–6218. [[CrossRef](#)]
31. Kuhn, A.; von Eschwege, K.G.; Conradie, J. Reduction Potentials of Para-Substituted Nitrobenzenes—an Infrared, Nuclear Magnetic Resonance, and Density Functional Theory Study. *J. Phys. Org. Chem.* **2012**, *25*, 58–68. [[CrossRef](#)]
32. Kuhn, A.; Conradie, J. Electrochemical and Density Functional Theory Study of Bis(Cyclopentadienyl) Mono(β -Diketonato) Titanium(IV) Cationic Complexes. *Electrochim. Acta* **2010**, *56*, 257–264. [[CrossRef](#)]
33. Kuhn, A.; Conradie, J. Orbital Control over the Metal vs. Ligand Reduction in a Series of Neutral and Cationic Bis(Cyclopentadienyl) Ti(IV) Complexes. *New J. Chem.* **2018**, *42*, 662–670. [[CrossRef](#)]
34. Conradie, J. Redox Chemistry of Tris(β -Diketonato)Cobalt(III) Complexes: A Molecular View. *J. Electrochem. Soc.* **2022**, *169*, 046522. [[CrossRef](#)]
35. Liu, R.; Conradie, J. Tris(β -Diketonato)Chromium(III) Complexes: Effect of the β -Diketonate Ligand on the Redox Properties. *Electrochim. Acta* **2015**, *185*, 288–296. [[CrossRef](#)]

36. Freitag, R.; Conradie, J. Electrochemical and Computational Chemistry Study of Mn(β -Diketonato)₃ Complexes. *Electrochim. Acta* **2015**, *158*, 418–426. [[CrossRef](#)]
37. Conradie, M.M.; Conradie, J. Electrochemical Behaviour of Tris(β -Diketonato)Iron(III) Complexes: A DFT and Experimental Study. *Electrochim. Acta* **2015**, *152*, 512–519. [[CrossRef](#)]
38. Kuhn, A.; Conradie, J. Synthesis, Electrochemical and DFT Study of Octahedral Bis(β -Diketonato)-Titanium(IV) Complexes. *Inorg. Chim. Acta* **2016**, *453*, 247–256. [[CrossRef](#)]
39. Conradie, J.; Mateyise, N.G.S.; Conradie, M.M. Reduction Potential of β -Diketones: Effect of Electron Donating, Aromatic and Ester Groups. *South African J. Sci. Technol.* **2019**, *38*, 1.
40. Nadjo, L.; Savéant, J.M. Electrochemical Reduction of Substituted Benzophenones and Fluorenones in Media of Low Proton Availability Mechanism of the Reductive Cleavage of Bromo and Chloro Benzophenones. *J. Electroanal. Chem.* **1971**, *30*, 41–57. [[CrossRef](#)]
41. Elving, P.J.; Leone, J.T. Mechanism of the Electrochemical Reduction of Phenyl Ketones. *J. Am. Chem. Soc.* **1958**, *80*, 1021–1029. [[CrossRef](#)]
42. Suzuki, M.; Elving, P.J. Kinetics and Mechanism for the Electrochemical Reduction of Benzophenone in Acidic Media. *J. Phys. Chem.* **1961**, *65*, 391–398. [[CrossRef](#)]
43. Geske, D.H.; Maki, A.H. Electrochemical Generation of Free Radicals and Their Study by Electron Spin Resonance Spectroscopy; the Nitrobenzene Anion Radical. *J. Am. Chem. Soc.* **1960**, *82*, 2671–2676. [[CrossRef](#)]
44. Kemula, W.; Grabowski, Z.R.; Kalinowski, M.K. Electrochemical Method of Studying the Reactions of Free Ketyl Radicals. *Naturwissenschaften* **1960**, *47*, 514. [[CrossRef](#)]
45. Mtshali, Z.; von Eschwege, K.G.; Conradie, J. Redox Data of Tris(Polypyridine)Manganese(II) Complexes. *Data* **2022**, *7*, 130. [[CrossRef](#)]
46. Elgrishi, N.; Rountree, K.J.; McCarthy, B.D.; Rountree, E.S.; Eisenhart, T.T.; Dempsey, J.L. A Practical Beginner's Guide to Cyclic Voltammetry. *J. Chem. Educ.* **2018**, *95*, 197–206. [[CrossRef](#)]
47. Kissinger, P.T.; Heineman, W.R. Cyclic Voltammetry. *J. Chem. Educ.* **1983**, *60*, 702–706. [[CrossRef](#)]